

## Original Article

# Calcium sulfate cement combined with silica-based mesoporous material for bone regeneration: *in vitro* and *in vivo* study

Honglue Tan<sup>1,2\*</sup>, Shengbing Yang<sup>2\*</sup>, Weifeng Liu<sup>3</sup>, Pengyi Dai<sup>1</sup>, Tingting Tang<sup>2</sup>, Wuyin Li<sup>1</sup>

<sup>1</sup>Luoyang Orthopedics and Traumatology Institution, Luoyang Orthopedic-Traumatological Hospital, Luoyang, China; <sup>2</sup>Shanghai Key Laboratory of Orthopedic Implants, Department of Orthopedic Surgery, The Shanghai Ninth People's Hospital, School of Medicine, Shanghai Jiao Tong University, Shanghai, China; <sup>3</sup>Department of Orthopedic Surgery, Changzhou Wujin Hospital, Jiangsu University, Changzhou, China. \*Equal contributors.

Received June 20, 2016; Accepted August 15, 2016; Epub November 15, 2016; Published November 30, 2016

**Abstract:** Objective: One of the disadvantages of using CSC (calcium sulfate cement) *in vivo* is its weak osteogenic activity. Thus composite materials based on CSC have been recently studied. Silica-based mesoporous material (SBA-15) shows great potential for biological applications because of its functionalized surfaces and biocompatibility. We assumed that blending SBA-15 into CSC could improve the osteogenic activity of the CSC. Methods: SBA-15 was blended into CSC powder at a mass ratio of 5%, 10% and 20% to make a CSC/SBA composite. Four groups including CSC (pure CSC), CSC-5S (5% mass ratio), CSC-10S (10% mass ratio) and CSC-20S (20% mass ratio) group were designed. The cell adherence was assessed using the cell counting. The cell proliferation was determined by 3-(4,5-dimethylthiazol-2-yl)-2,5-diphenyltetrazolium bromide (MTT) assay. The osteogenic differentiation was evaluated using alkaline phosphatase (ALP) staining, alizarin red staining analysis, and the expression levels of osteogenic related genes, mainly *ALP*, collagen I (*COL1*), osteopontin and osteocalcin. An *in vivo* animal study was performed using the radius bone defect in a rabbit model. The micro computed tomography (CT) and histological evaluation were used to investigate bone formation. Results: The number of adhered cells on the CSC-10S and CSC-20S surface was higher than that on CSC and CSC-5S surface. The relative cell proliferation rate in CSC/SBA group was higher than that in CSC group. Compared with CSC and CSC-5S group, ALP staining in CSC-10S and CSC-20S group was increased. Alizarin red staining in the different CSC/SBA groups was higher than that in the CSC group. Higher expression levels of osteogenic differentiation-related genes were seen in cells grown on CSC/SBA composite. Micro CT and histological evaluation confirmed that CSC/SBA composite improved the efficiency of new bone formation in the bone defect. The above osteogenic activities were enhanced with increased mass ratio of SBA-15 in CSC/SBA composite. Conclusion: Incorporation of SBA-15 into CSC could greatly improve the osteogenic activity of CSC, implying the CSC/SBA composite are more beneficial to the bone repairing than pristine CSC.

**Keywords:** Calcium sulfate cement, SBA-15, osteogenic property

## Introduction

Reconstruction of the bone defect using bone filling material is a common practice in orthopedic surgery. A key aspect of the bone repairing procedure is the consistency between new bone formation and the resorption of the grafting material. Calcium sulfate cement (CSC), with its good biocompatibility, osteoconduction and moldability, is widely used to repair bone defects. However, one of the disadvantages of using CSC *in vivo* is that its resorption rate is faster than new bone formation [1-3]. According

to the literature reports, CSC can be completely resorbed within 4 to 8 weeks, and the rapid resorption may influence the quality of newly formed bone, thus decreasing the mechanical properties of the repaired bone structure and ultimately leading to the appearance of a new bone fracture [3-5]. Though the rapid degradation of CSC can be tailored by adjusting the grain morphology, its biological activity to promote cell attachment, proliferation, and osteogenic differentiation is not good [6, 7]. In order to meet the requirements of clinical bone repair, composite materials based on CSC have been

recently studied to optimize the degradation rates, the mechanical properties, and the biological activity of CSC, and satisfactory results are also obtained [8, 9].

For bone tissue engineering, mesoporous silica materials with pore sizes between 2-50 nm have attracted significant attention owing to their structural properties, including uniform and tunable pore size distribution, high specific surface area, and high pore volume [10]. These characteristics make the mesoporous silica materials greatly enhanced *in vitro* apatite mineralization, and present an excellent delivery capability for osteogenic growth factors and drugs [11]. In addition, mesoporous silica materials have also been reported to support cell adhesion, proliferation, and differentiation *in vitro* [12]. As one kind of the silica-based mesoporous materials, SBA-15 showed potential for new biological applications because of its uniformly distributed nanopores, functionalized surfaces, and good biocompatibility [13]. Compared with the traditional nonmesoporous materials, SBA-15 has good bioactivity, which may promote the rapid formation of carbonated hydroxyapatite layers on its surface after soaking in simulated body fluids (SBF) [7]. Moreover, the ordered mesoporous channels of SBA-15 are also capable of loading large amounts of drugs, presenting great potential for applications in bone regeneration [14, 15]. In addition, preparation methods of these mesoporous materials has been optimized allowing mass production [14, 15].

In order to overcome the defects of the CSC, we prepared CSC/SBA composite materials by blending SBA-15 into CSC with different mass ratio. An *in vitro* study has showed that the physical performance of CSC/SBA significantly improved, such as the compressive strength, the ability to adsorb BMP-2, and the degradation rates [7]. However, the impact of CSC/SBA composite on the biological behavior of the osteogenic cells as well as the ability to repair bone defects *in vivo* still remains unknown. Therefore, the purpose of this study was to further explore the *in vitro* effect of CSC/SBA composite on the functions of human bone marrow mesenchymal stem cells (hMSCs), including the cell adhesion, proliferation, spreading and osteogenic differentiation, as well as to investigate the ability of the composite material to form new bone *in vivo* in a rabbit model with bone defect.

## Materials and methods

### Preparation of CSC/SBA

The powder component of CSC was calcium sulfate dihydrate (CSD;  $\text{CaSO}_4 \cdot 2\text{H}_2\text{O}$ , Reagent-Plus<sup>®</sup>,  $\geq 99\%$ ; Sigma-Aldrich). SBA-15 powder was kindly provided by Shengbing Yang (Engineering Research Center for Biomedical Materials of Ministry of Education, East China University of Science and Technology, Shanghai, China). SBA-15 was blended homogeneously into CSC powder at 0%, 5%, 10%, and 20% mass ratio. The blended powder was mixed with simulated body fluid (SBF) at a liquid to powder ratio (L/P) of 0.25 ml/4 g in a bowl until the powder achieved a homogenous paste. The obtained paste was transferred to a Teflon mold with a disc hole of 10 mm diameter and 3 mm height for *in vitro* cell study. For the animal study, the Teflon mold had a cylindrical hole of 6 mm diameter and 10 mm height. In both cases, the mold was then pressed between two metal plates for 24 hours. After the compound hardened, it was pulled out of the mold. The specimens were sterilized by gamma irradiation with 25 kGy of  $^{60}\text{Co}$  before use. According to the mass ratio of SBA-15, four groups were included in this study: CSC (no SBA-15), CSC-5S (5% mass ratio), CSC-10S (10% mass ratio), and CSC-20S (20% mass ratio) group.

### Cell culture

hMSCs were kindly provided by Shanghai Key Laboratory of Orthopedic Implants, and cultured as described in a previous study [16]. In brief, cells were cultured in  $\alpha$ -MEM culture medium supplemented with 10% fetal bovine serum (FBS), 1% penicillin ( $100 \text{ Uml}^{-1}$ ), and streptomycin sulphate ( $100 \text{ mg}\cdot\text{ml}^{-1}$ ) (GibcoBRL, Grand Island, NY). The cells were incubated at  $37^\circ\text{C}$  in a humidified atmosphere of 5%  $\text{CO}_2$  and 95% air, with the growth medium changed every 48 h until the cells reached 80-90% confluence. hMSCs passaged up to the third generation were used for the following experiments.

### Cell attachment and spreading

Cell attachment was evaluated as previously described [17, 18]. One milliliter of cell suspension with  $2 \times 10^4$  cells was seeded in a 48-well plate (Costar 3548, USA) that contained the

## CSC/SBA-15 composite for bone regeneration

different CSC/SBA discs and incubated at 37°C in a humidified atmosphere of 5% CO<sub>2</sub>. After 24 hours of cell culture, the cells on the substrate surface were gently washed three times with phosphate-buffered saline (PBS) and then fixed with 4% paraformaldehyde (PFA) for 15 min at room temperature. The cells were permeabilized with 0.1% Triton X-100 in PBS for 15 minutes, and then incubated with fluorescein isothiocyanate-phalloidin (Sigma-Aldrich) for 1 hour. After washing with PBS, the cell nuclei were stained with 4,6-diamidino-2-phenylindole (DAPI, Molecular Probe, Sigma-Aldrich). The cell numbers in five random fields were counted under a fluorescence microscope. The cells spreading were visualized and measured using confocal laser scanning microscopy (CLSM, Leica TCS SP2; Leica Microsystems, Heidelberg, German).

### *Cell proliferation*

Cell proliferation on the substrates was investigated using MTT assay after 1, 3, and 7 days of cell culture. Briefly, one milliliter of cell suspension with  $5 \times 10^3$  cells was seeded in 48-well plates (Costar 3548, USA) that contained different CSC/SBA discs and incubated at 37°C in a humidified atmosphere of 5%. A 48-well plate containing 1 ml of  $\alpha$ -MEM and CSC/SBA discs was used as a blank control. At the specified time points, 0.1 ml of the MTT solution (Sigma-Aldrich) was added to each well, and the plates were incubated for 4 h to form formazan. The supernatant was then discarded and 1 ml of dimethyl sulfoxide (DMSO, Sigma-Aldrich) was added to dissolve the formazan salts. The suspension containing formazan salts was transferred to another 48-well plate, and read at a wavelength of 570 nm using a microplate reader (Synergy HT, Biotek, Winooski, VT, USA). The mean OD values obtained from the blank control well were subtracted from the OD of the test groups. The modified OD values at day 3 and 7 were normalized to those at day 1 because the numbers of attached cells grown on different samples were different at day 1.

### *Osteogenic differentiation of hMSCs*

Cells were seeded at a density of  $3 \times 10^4$ /ml in 48-well plates containing CSC/SBA samples. After incubation for 24 hours, the culture medium was changed to the osteogenic induction culture medium containing Dulbecco's Modified Eagle Medium (DMEM; Hyclone, Thermo

Fisher Scientific Inc., Miami, FL, U.S.A.) supplemented with 10% fetal bovine serum (FBS; GibcoBRL, Grand Island, NY, U.S.A.), 1% penicillin (100 U/ml; GibcoBRL), streptomycin sulfate (100 mg/ml; GibcoBRL), 100  $\mu$ M dexamethasone, 50  $\mu$ M ascorbic acid, and 10 mM  $\beta$ -glycerophosphate sodium (Sigma-Aldrich). The osteogenic induction medium was replaced every two days.

After 7 and 14 days of culture, the substrates were washed three times with PBS, and then lysed in a 0.2% Triton X-100 solution through four standard freeze-thaw cycles. The ALP activity was performed according to the procedures reported in the literature [16]. After 14 days of culture, the ALP staining was accomplished following the procedures in the literature [19]. Briefly, the cells on the substrates were detached with 0.25% trypsin solution and removed to another 48-well plate containing 1 mL culture media. After 24-hour culture, the cells spread on the bottom of the wells. Then according to the procedures provided by the ALP staining kit (Renbao, Shanghai, People's Republic of China), the cells were rinsed twice with PBS, and fixed using buffered formalin for 30 seconds. After removing the formalin and washing with PBS, the cells were treated with a staining reagent for 60 minutes. Stained cells were photographed using a microscope (TE2000U; Nikon, Tokyo, Japan).

After 14 and 28 days incubation in osteogenic induction culture medium, the cells on the samples were fixed in 4% PFA for 15 min and stained with 1% alizarin red solution (Sigma-Aldrich) for 45 min at room temperature. The samples were then washed with PBS and dried at 37°C. Samples that were not seeded with cells were stained with alizarin red solution as a blank control. The images were then obtained using a digital camera (Nikon D90, Japan). After 28 days incubation in osteogenic induction culture medium, the quantitative analysis of the alizarin red was accomplished following the procedure in the literature [20]. In brief, the cells on the samples were fixed in 4% PFA for 15 min and stained with 1% alizarin red solution (Sigma-Aldrich) for 45 min at room temperature. The samples were then washed with PBS and the staining was dissolved in 10% cetylpyridinium chloride (Sigma-Aldrich), and the ODs were measured at a wavelength of 620 nm using a microplate reader (Synergy HT, Bio-Tek).

## CSC/SBA-15 composite for bone regeneration

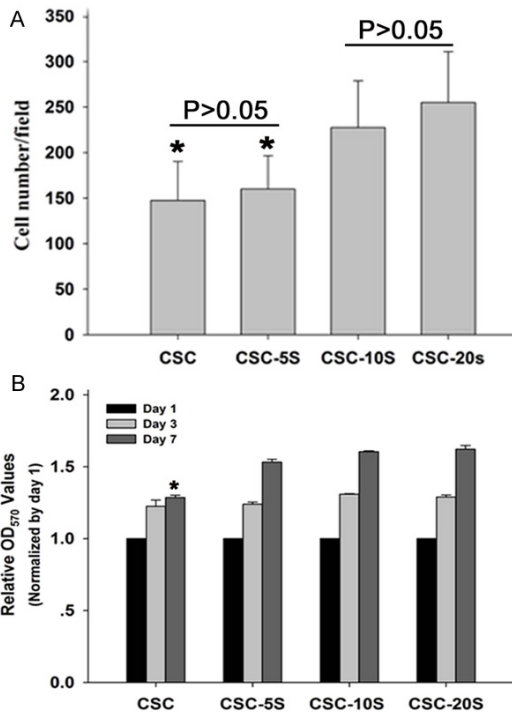


**Figure 1.** Attachment and proliferation of hMSC. A: Cell number of attachment. \* $P < 0.05$  vs. CSC-10S and CSC-20S. B: The relative proliferation rate. Each group displayed an increasing tendency from day 1 to day 7. \* $P < 0.05$  vs. CSC-5S, CSC-10S and CSC-20S at day 7.

### Quantitative real-time polymerase chain reaction (PCR)

hMSCs were seeded onto four specimens in 48-well plates at a density of  $3 \times 10^5$  cells/well and harvested after culture in osteogenic induction medium for 7, 14, and 21 days. The mRNA expression of osteogenic differentiation-related genes, h-alkaline phosphatase (*h-ALP*), h-collagen type I (*h-COL1*), h-osteopontin (*h-OPN*), and h-osteocalcin (*h-OC*), were quantitatively determined via real-time PCR. Total RNA was isolated from hMSCs grown on the samples using the TRIzol reagent (Invitrogen, Carlsbad, CA) according to the manufacturer's protocol. Quantitative real-time PCR was performed using an ABI 7500 Real-Time PCR System (Applied Biosystems, USA) with a PCR kit (SYBR Premix EX Taq, TaKaRa). The expression of the housekeeping gene glyceraldehyde-3-phosphate dehydrogenase (*h-GAPDH*) was used as an internal control to normalize the transcription levels of the genes results. The primers used for RT-qPCR were synthesized commercially and as follows: *h-COL*, forward

5'-CCTGAGCCAGCAGATCGAGAA-3', reverse 5'-GGTACACGCAGGTCTCACCAGT-3'; *h-ALP*, 5'-TTGACCTCCTCGGAAGACTC-3', reverse 5'-CCATACAGGATGGCAGTGAAGG-3'; *h-OPN*, 5'-CTGACGCGCCTTCTGATTG-3', reverse 5'-ACATCGGAATGCTCATTGCTCT-3'; *h-OC*, 5'-GGCGCTACCTGTATCAATGGC-3', reverse 5'-TGCCTGGAGAGGAGCAGAACT-3'; *h-GAPDH*, 5'-CCTGCACCACCACTGCTTA-3', reverse 5'-AGGCCATGCCAGTGAGCTT-3'.

### In vivo bone formation

In order to assess the ability of the materials to promote bone tissue regeneration, the radius bone defect in a rabbit model was used as animal model [21]. Surgical procedures and animal care were performed according to the institutional guidance of Luoyang orthopedics on animal experiment. All experiments were approved by the local animal welfare committee. Twenty-four adult female New Zealand White rabbits ( $2.86 \pm 0.20$  kg) were used. Surgery was performed under general anesthesia via weight-adapted intramuscular injection of 2% xylazine (12 mg/kg body weight) and ketamine (80 mg/kg body weight). The animals were placed in a supine position on sterile drapes, and their bodies were covered with sterile sheets. The right front limb was shaved, and the skin was cleaned with betadine. A longitudinal incision was made along the forearm skin. The periosteum was incised to approach to the radius bone. A critical sized defect of 10 mm in length was created at the middle position of the radius bone by using a high-speed micromotor. The different samples with 6 mm diameter and 10 mm height were implanted into the defect, and the periosteum was repositioned with an absorbable suture. The wound was then closed with a non-absorbable suture. The number of animals per group was six.

After two months, the rabbits were euthanized and the radius was excised and fixed in a 1.5% phosphate buffered glutaraldehyde solution. The radius was scanned using a Micro CT (X-RAY CT System, SMX-100CT-SV3 TYPE; Shimadzu Ltd, Kyoto, Japan). Images were reconstructed and analyzed using the Analyze software package (Biomedical Imaging Resource; Mayo Clinic, Rochester, MN, USA). After CT analysis, the specimen were dehydrated in a graded series of alcohol and

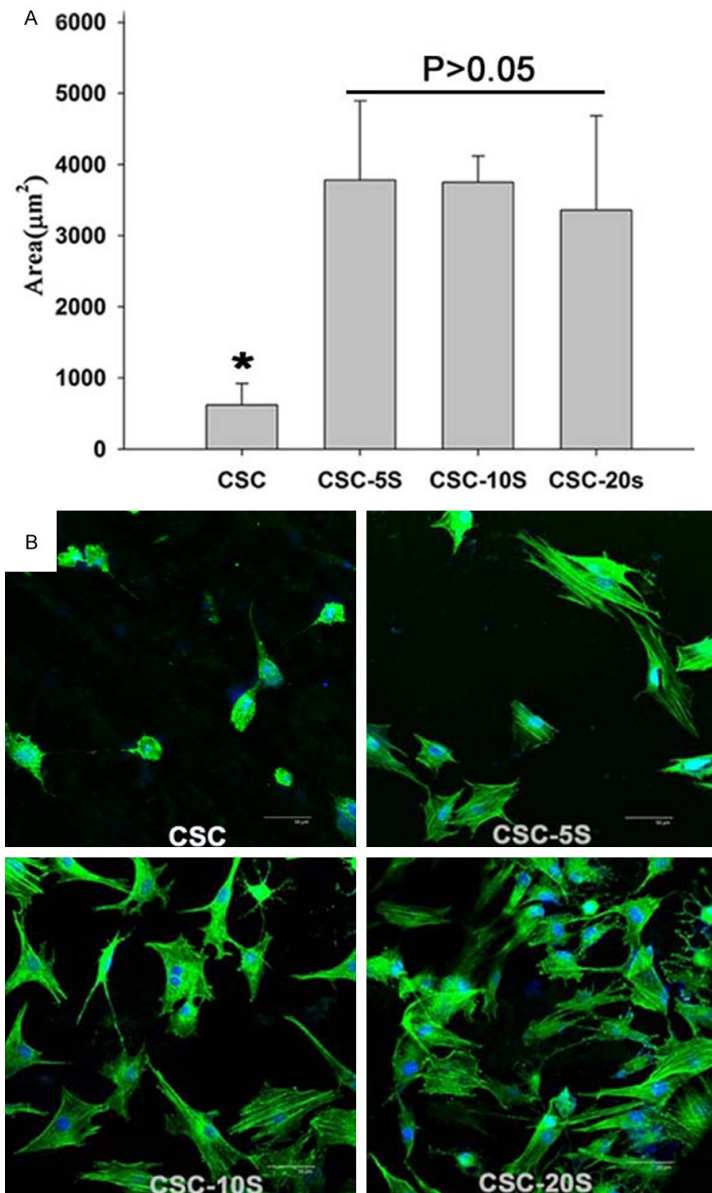


**Figure 2.** Morphology of hMSC. A: The spreading area. \* $P < 0.05$  vs. CSC-5S, CSC-10S and CSC-20S. B: Images of cells stained with rhodamine phalloidin for actin filaments (green) and nuclei counterstained with DAPI (blue).

embedded in methacrylate for histological analysis. Sections were stained with hematoxylin and eosin staining and picrofuchsin staining for evaluation of new bone formation.

#### Statistical analysis

All quantitative data were expressed as the mean  $\pm$  standard deviation. Statistical analysis was performed with one-way analysis of variance. All the data analyses were carried out

using SPSS software (SPSS 14.0, IBM Corporation, Armonk, NY, USA). A value of  $P < 0.05$  was considered statistically significant.

#### Results

##### Cell attachment and proliferation

The number of adherent cells on CSC-10S or CSC-20S were higher than that on the CSC or CSC-5S samples ( $P < 0.05$ ), no statistical differences were found between the CSC and CSC-5S, as well as between the CSC-10S and CSC-20S groups ( $P > 0.05$ , **Figure 1A**). The relative cell proliferation rate in each group displayed an increasing tendency from day 1 to day 7, presenting statistical differences among the three time points ( $P < 0.05$ ). The relative cell proliferation rate in CSC-5S, CSC-10S and CSC-20S groups was higher than that in CSC group at day 7 ( $P < 0.05$ , **Figure 1B**).

##### Cell spreading

The mean cell area on CSC, CSC-5S, CSC-10S and CSC-20S was  $620.25 \pm 302.37$ ,  $3780.50 \pm 1113.06$ ,  $3750.00 \pm 369.68$ , and  $3357.50 \pm 1326.61 \mu\text{m}^2$ , respectively. Compared with CSC-5S, CSC-10S and CSC-20S group, the cell spreading area on CSC surface was considerably smaller (**Figure 2A**). The cells on CSC-5S, CSC-10S and CSC-20S composite presented polygonal and spread morphology, whereas cells on CSC surface displayed a spherical morphology. Cells on CSC-20S surface also exhibited clustering and confluent morphology (**Figure 2B**).

##### Differentiation of hMSCs

hMSCs in CSC and CSC-5S group presented lower ALP activity than that in CSC-10S and CSC-20S group at day 7 ( $P < 0.05$ ). No differences were observed between CSC and CSC-5S group, as well as CSC-10S and CSC-20S

## CSC/SBA-15 composite for bone regeneration

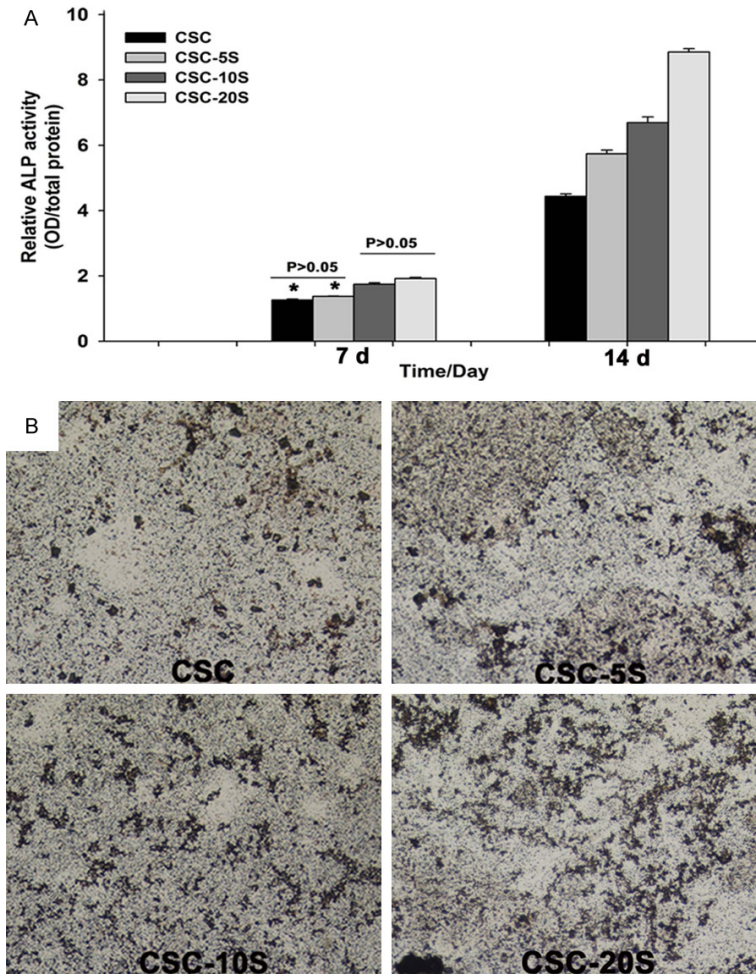


**Figure 3.** ALP activity and staining assay. A: Relative ALP activity. \* $P < 0.05$  vs. CSC-10S and CSC-20S at day 7. There existed significant differences between any two groups at day 14 ( $P < 0.05$ ). B: ALP staining on CSC/SBA composite at day 14.

group. At day 14, ALP activity levels in CSC, CSC-5S, CSC-10S, and CSC-20S group increased, presenting significant differences between any two groups ( $P < 0.05$ ) (Figure 3A). The positive ALP staining on CSC-10S and CSC-20S surface was stronger than that on CSC and CSC-5S surface at day 14 (Figure 3B).

CSC-10S and CSC-20S group exhibited higher mineralization than CSC and CSC-5S group at day 14 ( $P < 0.01$ ). The amount of mineralization in CSC-5S, CSC-10S and CSC-20S group at day 28 was higher than that in CSC group ( $P < 0.01$ ). No differences were found among CSC-5S, CSC-10S and CSC-20S group (Figure 4A). The alizarin red staining was similar on CSC-5S, CSC-10S and CSC-20S surface, and was considerably stronger than that on CSC surface at day 28 (Figure 4B).

### Expression of osteogenic differentiation-related genes

The expression of *h-COL1*, *h-ALP*, *h-OPN* and *h-OC* mRNA increased from day 7 to day 14. At day 21, the expression of *h-COL1*, *h-ALP* and *h-OPN* mRNA decreased, while *h-OC* mRNA expression continued to increase. At day 7, CSC-10S and CSC-20S group showed higher expression levels of *h-COL1* compared with CSC and CSC-5S group; CSC-5S, CSC-10S and CSC-20S group showed higher expression level of *h-ALP*, *h-OPN* and *h-OC* compared with CSC group. At day 14, compared with CSC group, CSC-5S, CSC-10S and CSC-20S group exhibited higher levels of *h-COL1*, *h-ALP*, *h-OPN* and *h-OC* expression, and the gene expression levels increased with increasing the SBA-15 mass ratio in CSC/SBA composite. At day 21, the highest expression levels of all genes were still found in CSC-20S group (Figure 5).

### In vivo animal study

The CSC group had the lowest bone binding, with less new bone formation in the bone defect; CSC-5S group was comparatively better than CSC group in bone integrity but still presented low bone formation. Nevertheless, both CSC-10S and CSC-20S group exhibited good bone bridging and healing, showing that CSC-20S group performed slightly better than CSC-10S group (Figure 6A). The regenerated bone mineral content (BMC) and bone mineral density (BMD) of the defect area were calculated to further quantitatively analyze the ability to promote bone formation. An increase in BMC values was observed for CSC/SBA composite which was dependent on the amount of SBA-15 incorporated, among which CSC-10S and CSC-20S group had much higher BMC than CSC and CSC-5S groups (Figure 6B). BMD values implied a similar profile, with the lowest

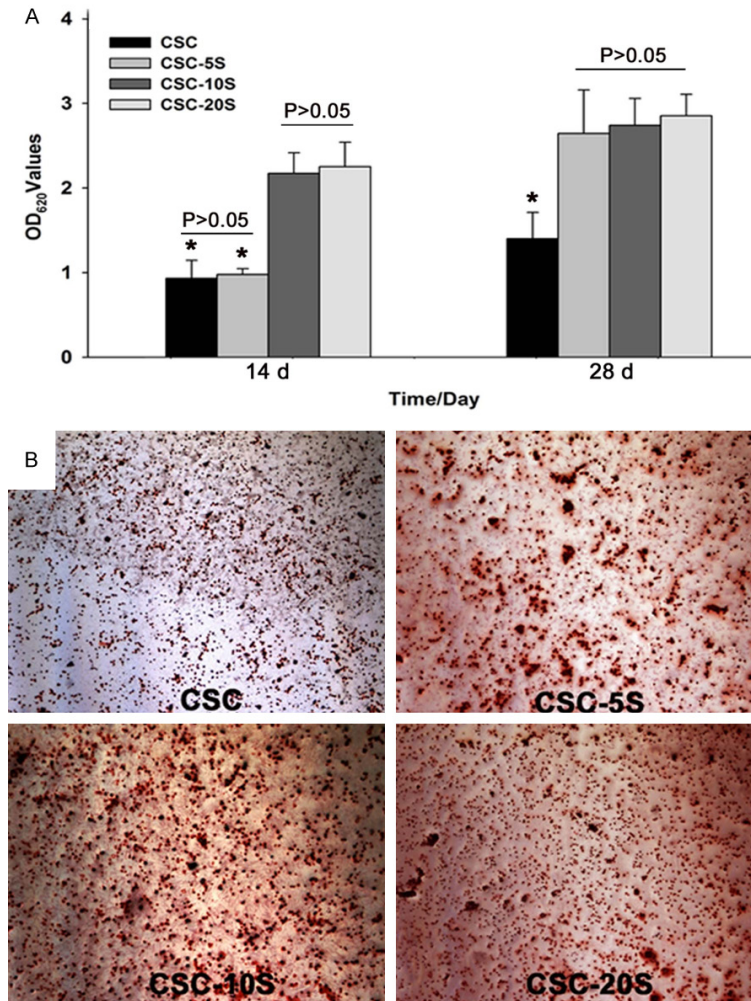


**Figure 4.** Alizarin red staining assay. A: At day 14, \* $P < 0.01$  vs. CSC-10S and CSC-20S. At day 21, \* $P < 0.01$  vs. CSC-5S, CSC-10S and CSC-20S. B: Colorimetric quantitative analysis of the extracellular matrix mineralization on the sample surface at day 21.

being found in CSC group and the highest in CSC-20S group (Figure 6C).

In CSC group, extensive fibrous connective tissues were observed in the bone defect site, in which few bone trabeculae appeared (Figure 7A, 7B). In CSC-5S group, more new bone formation was seen at the defect site although fibrous connective tissues were also present (Figure 7C and 7D). For CSC-10S and CSC-20S group, the bone defect was mostly filled by dense woven bone trabeculae. It is worth highlighting that the CSC-20S group surpassed CSC-10S group in bone formation (Figure 7E-H).

### Discussion

In addition to good physical and biomechanical performance, biomaterial used for bone

graft should possess the following features: osteoconduction, which provides scaffold for the creeping substitution of new bone, and osteogenic activity, which induces the differentiation of the pluripotent stem cell in surrounding tissue to the osteogenic cells [22]. Based on the deficiencies of CSC and the merits of the mesoporous silica material, the novel CSC/SBA composite was synthesized. The osteogenic activities of CSC/SBA were further investigated in this study, and found that the composite was more beneficial to the adhesion, spreading, and proliferation of hMSCs on the surface compared to the pristine CSC, and the biocompatibility of the composite was enhanced with increasing the mass ratio of SBA-15. This may be due to the increase of biological activity of composite material after combining CSC with ordered mesoporous silicon-based material SBA-15, which was in accordance with the results of mesoporous silica material reported in the literature [23-26].

Besides the initial adhesion and proliferation, the subsequent osteogenic differentiation of hMSCs is also important for the bone repair promoted by the biomaterial [27]. As an enzyme, ALP is an early marker of the differentiation of hMSCs to osteoblasts, whereas alizarin red is a late marker of the osteogenic differentiation [28]. Compared with the pristine CSC, the introduction of mesoporous SBA-15 into CSC can obviously increase the osteogenic activity of CSC/SBA. Cells on the composite surface expressed stronger ALP staining and higher mineralization in cell matrix, and the osteogenic activity of CSC/SBA also increased with the increase of mesoporous material mass ratio, which indicated that SBA-15 was more beneficial to the osteogenic differentiation of hMSCs.

## CSC/SBA-15 composite for bone regeneration

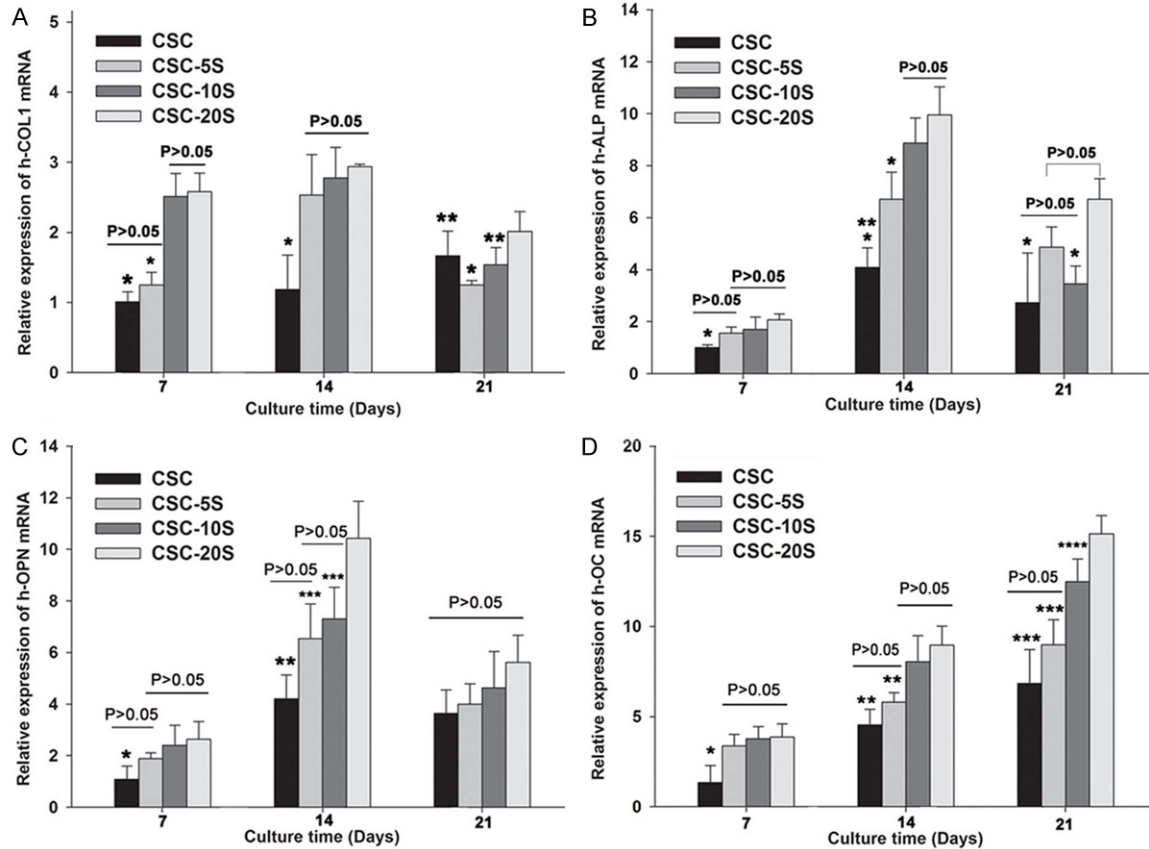


**Figure 5.** Relative gene expressions. A: *h-COL1* gene. \* $P < 0.01$  vs. CSC-10S and CSC-20S at day 7. \* $P < 0.01$  vs. CSC-5S, CSC-10S and CSC-20S at day 14. \* $P < 0.01$ , \*\* $P < 0.05$  vs. CSC-20S at day 21. B: *h-ALP* gene. \* $P < 0.05$  vs. CSC-10S and CSC-20S at day 7. \* $P < 0.05$  vs. CSC-10S and CSC-20S; \*\* $P < 0.05$  vs. CSC-5S, CSC-10S and CSC-20S at day 14. \* $P < 0.05$  vs. CSC-20S at day 21. C: *h-OPN* gene. \* $P < 0.05$  vs. CSC-10S and CSC-20S at day 7. \*\* $P < 0.05$  vs. CSC-10S and CSC-20S; \*\*\* $P < 0.05$  vs. CSC-20S at day 14. D: *h-OC* gene. \* $P < 0.05$  vs. CSC-5S, CSC-10S and CSC-20S at day 7. \*\* $P < 0.05$  vs. CSC-10S and CSC-20S at day 14. \*\*\* $P < 0.05$  vs. CSC-10S and CSC-20S; \*\*\*\* $P < 0.05$  vs. CSC-20S at day 21.

In order to further verify the aforementioned results, real-time PCR was used to detect the expression level of osteogenic differentiation-related genes at different time points. With respect to the CSC group, hMSCs in CSC-5S, CSC-10S and CSC-20S group showed higher *ALP*, *COL1* and *OP* expression level from day 7 to day 14. Though the expression levels showed a decreasing trend after 21 days, they were still higher than that in CSC group. As for *h-OC* gene, CSC-10S and CSC-20S group manifested high expression during cell culture. Meanwhile, the gene expression levels were also increased with increasing the mass ratio of SBA-15. The results further indicated that CSC/SBA composite was more conducive to the osteogenic differentiation of hMSCs than the pristine CSC.

In this study, we also compared the *in vivo* effect of CSC/SBA composite on osteogenesis by implanting the materials into defects produced in the radius of New Zealand rabbits. The micro CT and histological analyses confirmed that CSC-10S and CSC-20S group showed higher bone union and denser woven bone formation after 2 months implantation, and that CSC-20S materials were superior to CSC-10S group. However, CSC and CSC-5S group exhibited extensive fibrous connective tissues and few bone formation in the defect. The *in vivo* findings confirmed that CSC/SBA composite exhibited high efficiency for bone regeneration.

Recent research on mesoporous materials for bone regeneration mainly focused on the biological behavior of the material to osteoblast.

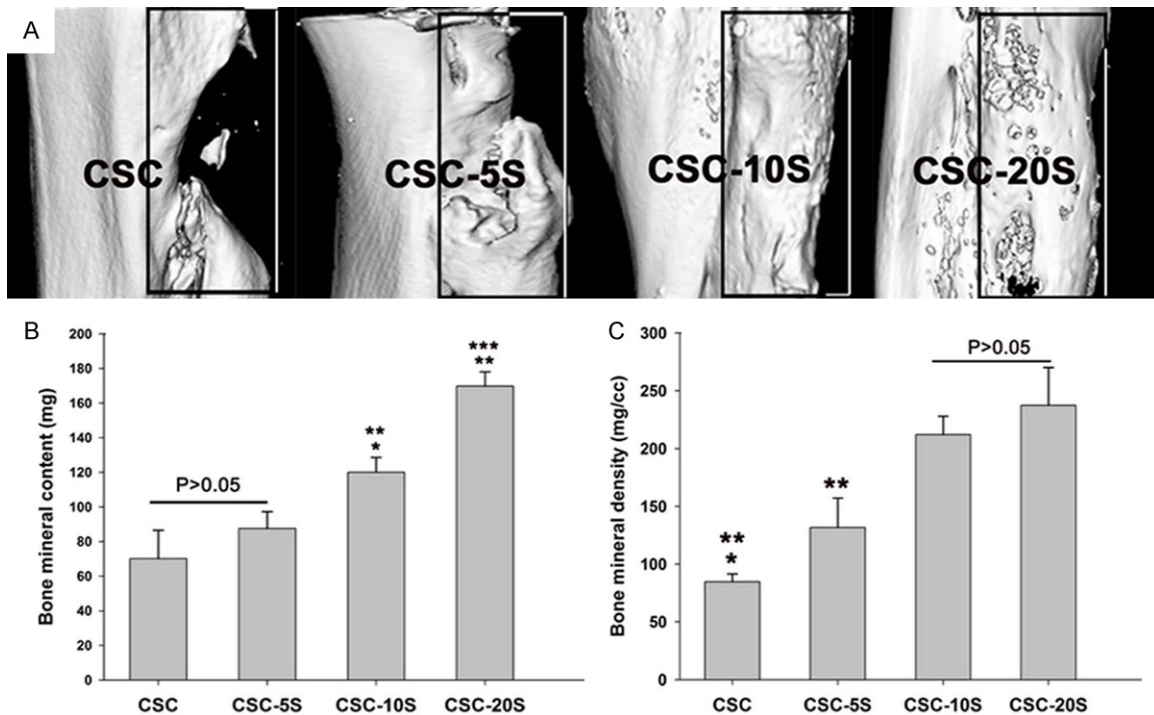


**Figure 6.** Micro CT images and quantitative data of bone formation. A: Three-dimensional Micro CT images. The boxed region in photograph represent the location of the radius bone defect. B: Bone mineral content (BMC). \* $P < 0.05$  vs. CSC-5S. \*\* $P < 0.01$  vs. CSC and CSC-5S. \*\*\* $P < 0.05$  vs. CSC-10S. C: Bone mineral density (BMD). \* $P < 0.05$  vs. CSC-5S. \*\* $P < 0.01$  vs. CSC-10S and CSC-20S.

A series of novel mesoporous bioactive glasses with different pore diameters and compositions have been synthesized, and their potential to promote proliferation and differentiation of osteoblast was superior to the ordinary bioactive glasses [29]. The mesoporous silica-based xerogels, which are mainly composed of a Si-O skeleton, possessed huge specific surface area, regular mesoporous channel and good biodegradation, which were then shown to promote the biological activity of osteoblast [30]. In addition, the silica-based xerogel combined with carbonate and phosphate was shown to greatly improve the osteoblast behavior by controlling the release rates of Ca, P and Si ions [30]. Radin et al. have shown that the dissolution speed of Si decreased by 25% after the deposition of carbonate and calcium phosphate on the surface of silica-based xerogel, and the active calcium phosphate layer can promote the adsorption of proteins, especially for the sticky protein, which can enhance the adhesive capacity of the cell on the material surface [31]. On the other hand, Ca and P can induce the proliferation and osteogenic differentiation

of bone marrow mesenchymal cells [31]. Some scholars also found that the formation of hydroxylapatite on the surface of silica-based xerogel was obviously accelerated due to the huge specific surface area, and thus the biological activity of xerogel surface was greatly improved [32]. In our study, the *in vitro* research showed that the CSC/SBA composite with the introduction of mesoporous SBA-15 was more favorable to hMSC adhesion, proliferation and differentiation to the osteoblast than pure calcium sulfate. The results were in accordance with the literature reports in which the performance of the self-curing material composited by calcium sulfate, dicalcium silicate and tricalcium silicate showed improved mechanical properties, osteogenic activity and degradation compared with CSC [33]. Combined with the literature reports and the results in our work, the improvement of osteogenic activity of CSC/SBA may be related with the ionic composition and physical properties of ordered mesoporous material SBA-15.

In conclusions, incorporation of SBA-15 into CSC could greatly improve the osteogenic activ-

## CSC/SBA-15 composite for bone regeneration

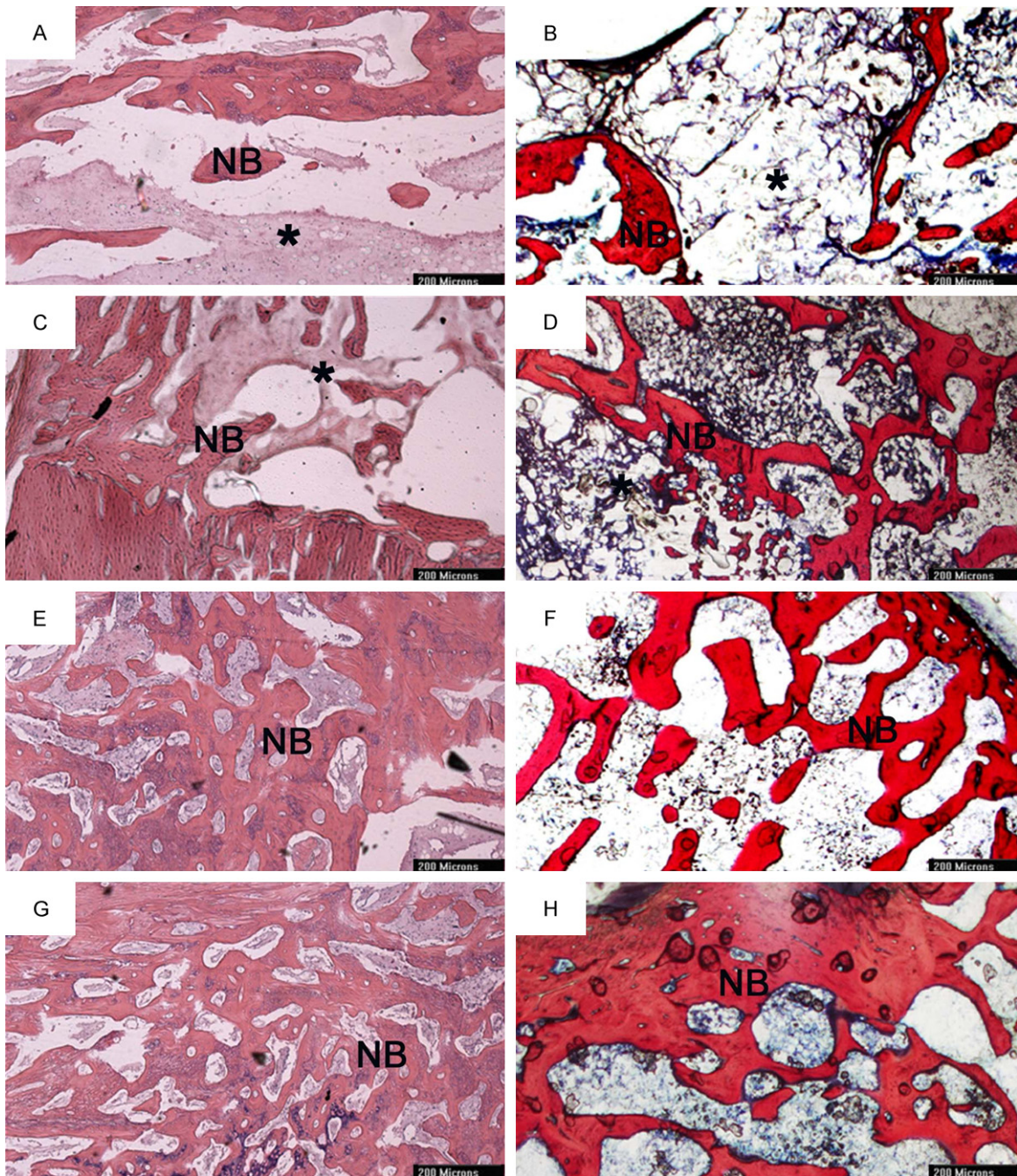


**Figure 7.** Histological evaluation. A, C, E and G are HE staining. B, D, F and H are picro-fuchsin staining. Pure CSC (A, B). CSC-5S (C, D). CSC-10S (E, F). CSC-20S (G, H). NB, new bone. Asterisk represent the fibrous connective tissues.

ity of calcium sulfate cement, which was more favorable to hMSC adhesion, proliferation and osteogenic differentiation than pristine CSC. Micro CT and histological evaluations confirmed that CSC/SBA promoted new bone formation in the bone defect. The osteogenic activities of CSC/SBA composite were enhanced with increasing mass ratio of the SBS-15.

Thus, The CSC/SBA composite are more beneficial to the bone repairing than pristine CSC.

### Acknowledgements

This study was supported by the Opening Project of Shanghai Key Laboratory of Orthopaedic Implants (KFKT2016002).

**Disclosure of conflict of interest**

None.

**Address correspondence to:** Wuyin Li, Luoyang Orthopedics and Traumatology Institution, Luoyang Orthopedic-Traumatological Hospital, Luoyang, Henan Province, China. E-mail: 15036358806@163.com

**References**

- [1] Vallet-Regí M, González-Calbet JM. Calcium phosphates as substitution of bone tissues. *Prog Solid State Chem* 2004; 32: 1-31.
- [2] Hu GF, Xiao LW, Fu H, Bi DW, Ma HT, Tong PJ. Study on injectable and degradable cement of calcium sulphate and calcium phosphate for bone repair. *J Mater Sci Mater Med* 2010; 21: 627-34.
- [3] Bu BX, Wang MJ, Liu WF, Wang YS, Tan HL. Short-segment posterior instrumentation combined with calcium sulfate cement vertebroplasty for thoracolumbar compression fractures: radiographic outcomes including nonunion and other complications. *Orthop Traumatol Surg Res* 2015; 101: 227-33.
- [4] Hing KA, Wilson LF, Buckland T. Comparative performance of three ceramic bone substitutes. *Spine* 2007; 7: 475-90.
- [5] Oner FC, Van der Rijt RR, Ramos LM, Dhert WJ, Verbout AJ. Changes in the disc space after fractures of the thoracolumbar spine. *J Bone Joint Surg Br* 1998; 80: 833-9.
- [6] Yang GJ, Lin M, Zhang L, Gou ZR. Progress of calcium sulfate and inorganic composites for bone defect repair. *J Inorgan Mater* 2013; 28: 795-803.
- [7] Tan HL, Yang SB, Dai PY, Li WY, Yue B. Preparation and physical characterization of CSC/SBA composites for controlled release of BMP-2. *Int J Nanomed* 2015; 10: 4341-50.
- [8] Borhan S, Hesarakı S, Ahmadzadeh-Asl S. Evaluation of colloidal silica suspension as efficient additive for improving physicochemical and in vitro biological properties of calcium sulfate-based nanocomposite bone cement. *J Mater Sci Mater Med* 2010; 21: 3171-81.
- [9] Nilsson M, Zheng MH, Tägil M. The composite of hydroxyapatite and calcium sulphate: a review of preclinical evaluation and clinical applications. *Expert Rev Med Devices* 2013; 10: 675-84.
- [10] Tabasi O, Falamaki C, Khalaj Z. Functionalized mesoporous silicon for targeted-drug-delivery. *Colloids Surf Biointerfaces* 2012; 98: 18-25.
- [11] Vallet-Regí M, Ruiz-Hernandez E. Bioceramics: from bone regeneration to cancer nanomedicine. *Adv Mater* 2011; 23: 5177-218.
- [12] Rosenholm JM, Sahlgrén C, Lindén M. Towards multifunctional, targeted drug delivery systems using mesoporous silica nanoparticles-opportunities & challenges. *Nanoscale* 2010; 2: 1870-83.
- [13] Zhao D, Feng J, Huo Q, Melosh N, Fredrickson GH, Chmelka BF, Stucky GD. Triblock copolymer syntheses of mesoporous silica with periodic 50 to 300 angstrom pores. *Science* 1998; 279: 548-52.
- [14] Shadjou N, Hasanzadeh M. Silica-based mesoporous nanobiomaterials as promoter of bone regeneration process. *J Biomed Mater Res A* 2015; 103: 3703-16.
- [15] Qian M, Liu M, Duan M, Wu Z, Zhou Y. Synthesis of composites SBA-15 mesoporous particles carrying oxytocin and evaluation of their properties, functions, and in vitro biological activities. *Cell Biochem Biophys* 2015; 71: 127-34.
- [16] Sun HL, Wu CT, Dai KR, Chang J, Tang TT. Proliferation and osteoblastic differentiation of human bone marrow-derived stromal cells on akermanite bioactive ceramics. *Biomaterials* 2006; 27: 5651-57.
- [17] Moutzouri AG, Athanassiou GM. Attachment, Spreading, and Adhesion Strength of Human Bone Marrow Cells on Chitosan. *Ann Biomed Eng* 2011; 39: 730-41.
- [18] Zhao LZ, Mei SL, Chu PK, Zhang YM, Wu ZF. The influence of hierarchical hybrid micro/nano-textured titanium surface with titania nanotubes on osteoblast functions. *Biomaterials* 2010; 31: 5072-82.
- [19] Yang SB, Xu SG, Zhoy PY, Wang J, Tan HL, Liu Y, Tang TT, Liu CS. Siliceous mesostructured cellular foams/poly(3-hydroxybutyrate-co-3-hydroxyhexanoate) composite biomaterials for bone regeneration. *Int J Nanomed* 2014; 9: 4795-807.
- [20] Tan HL, Guo SR, Yang SB, Xu XF, Tang TT. Physical characterization and osteogenic activity of the quaternized chitosan-loaded PMMA bone cement. *Acta Biomaterialia* 2012; 8: 2166-74.
- [21] Li Y, Chen SK, Li L, Qin L, Wang XL, Lai YX. Bone defect animal models for testing efficacy of bone substitute biomaterials. *Journal of Orthopaedic Translation* 2015; 3: 95-104.
- [22] Cypher TJ, Grossman JP. Biological principles of bone graft healing. *J Foot Ankle Surg* 1996; 35: 413-7.
- [23] Shi XT, Wang YJ, Ren L, Zhao NR, Gong YH, Wang DA. Novel mesoporous silica-based antibiotic releasing scaffold for bone repair. *Acta Biomaterialia* 2009; 5: 1697-707.
- [24] López-Noriega A, Arcos D, Izquierdo-Barba I, Sakamoto Y, Terasaki O, Vallet-Regí M. Ordered mesoporous bioactive glasses for bone tissue regeneration. *Chem Mater* 2006; 18: 3137-44.

## CSC/SBA-15 composite for bone regeneration

- [25] Trejo CG, Lozano D, Manzano M, Doadrio JC, Salinas AJ, Dapía S, Gómez-Barrena E, Vallet-Regí M, García-Honduvilla N, Buján J, Esbrit P. The osteoinductive properties of mesoporous silicate coated with osteostatin in a rabbit femur cavity defect model. *Biomaterials* 2010; 31: 8564-73.
- [26] Fan DM, Akkaraju GR, Couch EF, Canham LT, Coffey JL. The role of nanostructured mesoporous silicon in discriminating in vitro calcification for electrospun composite tissue engineering scaffolds. *Nanoscale* 2011; 3: 354-61.
- [27] Hu X, Neoh KG, Shi Z, Kang ET, Poh C, Wang W. An in vitro assessment of titanium functionalized with polysaccharides conjugated with vascular endothelial growth factor for enhanced osseointegration and inhibition of bacterial adhesion. *Biomaterials* 2010; 31: 8854-8863.
- [28] Moreau JL, Xu HH. Mesenchymal stem cell proliferation and differentiation on an injectable calcium phosphate-chitosan composite scaffold. *Biomaterials* 2009; 30: 2675-2682.
- [29] Yan XX, Wei GF, Zhao LZ, Yi J, Deng HX, Wang LZ, Lu GQ, Yu CZ. Synthesis and in vitro bioactivity of ordered mesostructured bioactive glasses with adjustable pore sizes. *Micropor Mesopor Mat* 2010; 132: 282-9.
- [30] Boury B, Corriu RJ, Delord P, Le Strat VL. Structure of silica-based organic-inorganic hybrid xerogel. *J Non-Cryst Solid* 2000; 265: 41-50.
- [31] Radin S, Falaize S, Lee MH, Ducheyne P. In vitro bioactivity and degradation behavior of silica xerogels intended as controlled release materials. *Biomaterials* 2002; 23: 3113-22.
- [32] Zhou HJ, Wu XH, Wei J, Lu X, Zhang S, Shi JL, Liu CS. Stimulated osteoblastic proliferation by mesoporous silica xerogel with high specific surface area. *J Mater Sci Mater Med* 2011; 22: 731-9.
- [33] Huang ZG, Chang J. Self-setting properties and in vitro bioactivity of calcium sulfate hemihydrate-tricalcium silicate composite bone cements. *Acta Biomaterialia* 2007; 3: 952-60.